(5) E. Benedetti, V. Pavone, C. Toniolo, G. M. Bonora, and M. Palumbo, *Macromolecules*, **10**, 1350 (1977).
(6) E. Benedetti in "Peptides", M. Goodman and J. Meienhofer, Ed., Wiley, New York, 1977, pp 257–273.
(7) C. Toniolo in "Bioorganic Chemistry", E. E. van Tamelen, Ed., Academic Press, New York, 1977, pp 265–291.
(8) C. Toniolo, *Crit. Rev. Biochem.*, in press.
(9) C. M. Deber, *Macromolecules*, **7**, 47 (1974).
(10) N. M. Galitsky, V. I. Deigin, W. Saenger, and V. Z. Pletnev, *Bioorg. Khim.*, **3**, 1445 (1977).
(11) J. Stezowski and R. E. Hughes, cited in J. C. Howard, F. A. Momany, R. H. Andreatta, and H. A. Scheraga, *Macromolecules*, **6**, 535 (1973).
(12) G. M. Bonora and C. Toniolo, *Gazz. Chim. Ital.*, **107**, 381 (1977).
(13) R. H. Wiley and O. H. Borum, *J. Am. Chem. Soc.*, **72**, 1626 (1950).
(14) G. Germain, P. Main, and M. M. Woolfson, *Acta Crystallogr., Sect. A*, **27**, 368 (1971).
(15) D. T. Cramer and J. T. Waber in "International Tables for X-Ray Crystallography", Vol. IV, The Kynoch Press, Birmingham, England, 1974, Table 2.2B.
(16) A. B. Mauger, W. J. Rzeszotarski, and R. A. Ford, *Org. Magn. Reson.*, **5**, 231 (1973).
(17) E. Benedetti, M. R. Ciajolo, and A. Maisto, *Acta Crystallogr., Sect. B*, **30**, 1783 (1974).
(18) R. Parthasarathy, B. Paul, and W. Korytnyk, *J. Am. Chem. Soc.*, **98**, 6634 (1976).
(19) E. Benedetti and C. Toniolo, manuscript in preparation.
(20) IUPAC-IUB Commission on Biochemical Nomenclature, *Biochemistry*, **9**, 3471 (1970).
(21) H. Itoh, T. Yamane, T. Ashida, T. Sugihara, Y. Imanishi, and T. Higashimura, *Acta Crystallogr., Sect. B*, **32**, 3355 (1976).
(22) R. E. Marsh, M. R. Narasimha Murthy, and K. Venkatesan, *J. Am. Chem. Soc.*, **99**, 1251 (1977).
(23) S. Kashino, T. Ashida, and M. Kakudo, *Acta Crystallogr., Sect. B*, **30**, 2074 (1974).
(24) R. E. Marsh and J. P. Glusker, *Acta Crystallogr.*, **14**, 1110 (1961).
(25) T. Ueki, T. Ashida, M. Kakudo, Y. Sasada, and Y. Katsube, *Acta Crystallogr., Sect. B*, **25**, 1840 (1969).
(26) F. Conti and P. De Santis, *Biopolymers*, **10**, 2581 (1971).
(27) R. Balasubramanian, A. V. Lakshminarayanan, M. N. Sabesan, G. Tegoni, K. Venkatesan, and G. N. Ramachandran, *Int. J. Pept. Protein Res.*, *3*, 25 (1971).
(28) T. Ashida and M. Kakudo, *Bull. Chem. Soc. Jpn.*, **47**, 1129 (1974).
(29) J. D. Dunitz and P. Strickler in "Structural Chemistry and Molecular Biology", A. Rich and N. Davidson, Ed., N. H. Freeman, San Francisco, Calif., 1968, pp 595–602.
(30) J. Mitra and C. Ramakhrishnan, *Int. J. Pept. Protein Res.*, **9**, 27 (1977).
(31) P. E. Young and C. M. Deber, *Biopolymers*, **14**, 1547 (1975).
(32) J. T. Bulmer and H. F. Shurvell, *J. Phys. Chem.*, **77**, 256 (1973).
(33) G. Boussard, M. Marraud, J. Néel, B. Maigret, and A. Aubry, *Biopolymers*, **16**, 1033 (1977).
(34) R. Wolfenden, *Biochemistry*, **17**, 201 (1978).
(35) During the preparation of the manuscript we became aware of a paper by K. Itoh, T. Yamane, and T. Ashida, *Acta Crystallogr.*, **34**, 2640 (1978), which also describes results of an independent X-ray diffraction analysis of *t*-Boc-L-Pro-Sar-OH. We were pleased to note that the overall conformation of the molecule and the details of the geometrical parameters reported by Japanese authors match closely those described in the present paper.

Polymer Diffusion in a Dilute Solution. 2. Poly[bis(*m*-chlorophenoxy)phosphazene] in Chloroform

B. Chu* and Esin Gulari

Chemistry Department, State University of New York at Stony Brook, Long Island, New York, 11794. *Received December 11, 1978*

ABSTRACT: Translational diffusion coefficients of poly[bis(*m*-chlorophenoxy)phosphazene] of known molecular weight distribution in chloroform at 25 °C have been studied using Rayleigh line-width spectroscopy. By combining light scattering intensity measurements where we determined the molecular weight $M_r = 3.45 \times 10^6$ g/mol, the second virial coefficient $A_2 = 1.39 \times 10^{-4}$ (cm^3 mol)/g^2, and the radius of gyration $\langle r_g^2 \rangle^{1/2} = 1.54 \times 10^3$ Å with the concentration dependence of the diffusion coefficient $k_D = 116$ g of solution/g or 78.4 cm^3/g, and the molecular weight dependence of radius of gyration $r_g = 2.89 \times 10^{-9} M^{0.57}$, we are able to make a transformation from Γ space to M space and to obtain the molecular weight distribution function from a histogram analysis of the photoelectron time correlation function of light scattered by the polymer solution at a finite concentration. Our molecular weight distribution function is in essential agreement with the GPC result. It should be noted that this new approach should enable determinations of molecular weight distribution functions of extremely high molecular weights ($\sim 10^9$ g/mol), not accessible by the GPC method. Furthermore, the method is nondestructive, needs only small quantities of the polymer solution, and, in principle, takes merely minutes for each measurement and analysis under most circumstances.

I. Introduction

The high molecular weight, open-chain poly(dichlorophosphazene) obtained from high-temperature melt polymerization of hexachlorocyclotriphosphazene is a thermally stable elastomer but lacks hydrolytic stability. Allcock[1] was able to substitute the reactive chlorine groups of poly(dichlorophosphazene) with a variety of organic nucleophiles. Aside from the earlier reviews by Allcock,[2,3] the synthesis, properties, and applications of polyphosphazenes have been reported[4] and reviewed[5] by members of the Army Materials and Mechanics Research Center at Watertown, Mass. Of the seven different poly(aryloxyphosphazene) homopolymers reported,[4] the molecular weight distribution of poly[bis(*m*-chlorophenoxy)phosphazene] (sample IIIe in ref 4) has been determined using a Waters ANAPREP gel permeation chromatograph.[6] In this article, we explore a new general approach to the determination of molecular weight distribution of linear poly(phosphazenes) using a well characterized poly[bis(*m*-chlorophenoxy)phosphazene] (sample IIIe in ref 4)[7] as an example. In section II, we shall provide the theoretical background for a generalized procedure in the determination of molecular weight distribution of polymer solutions by means of light-scattering spectroscopy. In sections III and IV, the experimental methods and procedures of data analysis will be outlined. Finally, we shall illustrate this new method by presenting the light scattering results of sample IIIe.

II. Theoretical Background

A. Light-Scattering Intensity Measurements. According to the Rayleigh–Gans–Debye theory,[8] the

0024-9297/79/2212-0445$01.00/0

Rayleigh ratio for vertically polarized light at finite concentrations has the form:[9]

$$\frac{HC}{R_{vv}} = \frac{1}{M_r P_1(K,C)} + 2A_2(C)\frac{P_2(K,C)}{P_1^2(K,C)}C + \dots \quad (1)$$

where $H = 4\pi^2 n_0^2 (\partial n/\partial C)^2/N_A\lambda_0^4$ with n_0, C, N_A, and λ_0 being the respective refractive index, the concentration, the Avogadro number, and the wavelength of light in vacuo; $R_{vv} = r^2 i_{vv}/I$ with R_{vv}, r, i_{vv}, and I being the Rayleigh ratio, the distance between the scattering center and the point of observation, the excess vertically polarized scattered intensity, and the incident intensity, respectively; M_r ($\equiv\sum_i C_i M_i/\sum_i C_i$) and A_2 are the weight-average molecular weight and the second virial coefficient; and $P_1(K,C)$ and $P_2(K,C)$ are the respective intramolecular and intermolecular interference factors. K ($\equiv(4\pi/\lambda)(\sin(\theta/2))$ is the magnitude of momentum transfer vector. At infinite dilution, $P_1(K,C) = P(K)$, and $P_2(K,C)/P_1^2(K,C) = 1$. Then

$$\lim_{C\to 0}\frac{HC}{R_{vv}} = \frac{1}{M_r P_1(K,C)} \quad (2)$$

At finite concentrations, if we take

$$P_1(K,C) = 1 - \frac{16\pi^2 n_0^2}{3\lambda_0^2}\langle r_g^2(C)\rangle_z \sin^2(\theta/2) \quad (3)$$

and $2A_2(C)[P_2(K,C)/P_1^2(K,C)]C \approx 2A_2C$, then eq 1 reduces to

$$\frac{HC}{R_{vv}} = \frac{1}{M_r}\left[1 + \frac{16\pi^2 n_0^2}{3\lambda_0^2}\langle r_g^2(C)\rangle_z \sin^2(\theta/2)\right] + 2A_2C$$

or

$$\frac{HC}{R_{vv}} = \left[\frac{1}{M_r} + 2A_2C\right]\times \left[1 + (1 + 2A_2CM_r)^{-1}\frac{16\pi^2 n_0^2}{3\lambda_0^2}\langle r_g^2(C)\rangle_z \sin^2(\theta/2)\right] \quad (4)$$

Thus, in a plot of HC/R_{vv} vs. $\sin^2(\theta/2)$,

$$\langle r_g^2(C)\rangle_z = \frac{\text{initial slope}}{\text{intercept}}(1 + 2A_2CM_r)\frac{3\lambda_0^2}{16\pi^2 n_0^2} \quad (5)$$

The terms A_2 and M_r can be determined from a plot of

$$\lim_{\theta\to 0}\frac{HC}{R_{vv}} \text{ vs. } C$$

where we have

$$\lim_{\theta\to 0}\frac{HC}{R_{vv}} = \frac{1}{M_r} + 2A_2C \quad (6)$$

Without referring to the $(1 + 2A_2CM_r)$ term, we shall define

$$\langle r_g^2(C)\rangle_z^* = \langle r_g^2(C)\rangle_z/(1 + 2A_2CM_r) \quad (7)$$

as an effective interference term.

B. Light-Scattering Line-Width Measurements. The translational diffusion coefficient for a dilute polymer solution can be expanded to first order in concentration as

$$D = D_0(1 + k_D C + \dots) \quad (8)$$

where

$$k_D \approx 2A_2M - (k_f F + \bar{v}) \quad (9)$$

with k_f, $\bar{v}$, and F being the first-order friction coefficient, the specific volume of the polymer, and a temperature-dependent constant, respectively. At infinite dilution,

$$D_0 = k_T M^{-b} \quad (10)$$

where $b = {}^1/_2$ at the Θ temperature. If we take the hydrodynamic volume of a polymer molecule V_h to be ${}^4/_3\pi r_h^3$ with r_h being the effective hydrodynamic radius and invoke the Stokes-Einstein relation $D_0 = k_B T/6\pi\eta r_h$ where k_B and η are the Boltzmann constant and the solvent viscosity, respectively, we get

$$V_h = \frac{4}{3}\pi\left[\frac{k_B T}{6\pi\eta k_T}\right]^3 M^{3b} \quad (11)$$

and

$$k_D = 2A_2M - \left[\bar{v} + \frac{4}{3}\pi N_A\left(\frac{k_B T}{6\pi\eta k_T}\right)^3 M^{3b-1}F\right] \quad (12)$$

In a dilute Θ solution at the Θ temperature,

$$k_D = -\bar{v} - \frac{4}{3}\pi N_A F\left(\frac{k_B T}{6\pi\eta k_T}\right)^3 M^{1/2} \quad (13)$$

where $F = 2.23$ and 1.0 according to the Pyun and Fixman theory[10] and the Yamakawa[11]–Imai[12] theory, respectively. In this study, we take k_D to be independent of molecular weight and use

$$D_0 \approx D/(1 + k_D C) \quad (14)$$

at dilute concentration where $D = \Gamma/K^2$ with Γ being the line width. Thus,

$$\frac{\Gamma}{K^2(1 + k_D C)} = k_T M^{-b} \quad (15)$$

Equation 15 forms the basis of our transformation from Γ space to M space, since we can write

$$M = \left[\frac{k_T K^2(1 + k_D C)}{\Gamma}\right]^{1/b} \quad (16)$$

The details of the transformation will be described in section IV.

III. Experimental Methods

Reagent grade chloroform was used without further purification. Dry poly[bis(*m*-chlorophenoxy)phosphazene] (sample IIIe in ref 4) was dissolved in chloroform. The solution was then passed through a Millipore filter (type FHLP, nominal pore size = 0.5 μm) directly into the light-scattering cell.

The detailed design of our light-scattering spectometers has been described elsewhere.[13,14] In the present experiment, we used an argon ion laser operating at 488.0 nm and 150 mW and a 96-channel single-clipped Malvern correlator for measurements of photoelectron-count autocorrelation function. Temperature at 25 °C was controlled to ±0.01 °C.

IV. Histogram Method of Data Analysis

By using the cumulants method, we can obtain only limited information on the line-width distribution function, because it is difficult to determine moments μ_i beyond the second moment μ_2, where

$$\mu_i = \int (\Gamma - \bar{\Gamma})^i G(\Gamma)\, d\Gamma \quad (17)$$

with $\bar{\Gamma} = \int G(\Gamma)\Gamma\, d\Gamma$ and $G(\Gamma)$ being the normalized distribution function of line widths.

In the histogram method,[15] we used a discrete step function (a histogram) to approximate $G(\Gamma)$, such that

$$\sum_{j=1}^{n} G(\Gamma_j)\Delta\Gamma = 1 \quad (18)$$

and

$$|g^{(1)}(\tau)| = \sum_{j=0}^{n} G(\Gamma_j) \int_{\Gamma_j-\Delta\Gamma/2}^{\Gamma_j+\Delta\Gamma/2} \exp(-\Gamma I\Delta\tau)\, d\Gamma \quad (19)$$

where $g^{(1)}(\tau)$ is the normalized correlation function of the scattered electric field, $G(\Gamma_j)$ is the total integrated scattered intensity of molecules having line widths from $\Gamma_j - \Delta\Gamma/2$ to $\Gamma_j + \Delta\Gamma/2$, n is the number of steps in the histogram, $\Delta\Gamma$ [$=(\Gamma_{max} - \Gamma_{min})/n$] is the width of each step, $\Delta\tau$ is the delay time increment, and I is the delay channel number with $\tau = I\Delta\tau$. Values for Γ_{min} and Γ_{max} signaling the start and stop of the range of the line-width distribution function are arbitrary. For example, we can set a step equal to zero when its contribution is less than 0.25% of an averaged step in $G(\Gamma)$. In this respect, the histogram method tends to neglect the effect of long tails and approximate $G(\Gamma)$ with a distribution function which has a sharper cut-off feature.

The nonlinear least-squares method minimizes χ^2 with respect to each a_j ($\equiv G(\Gamma_j)$) simultaneously, such that

$$\frac{\partial}{\partial a_j}\chi^2 = \frac{\partial}{\partial a_j}\sum\left\{\frac{1}{\sigma_I^2}[Y_m(I\Delta\tau) - Y(I\Delta\tau)]^2\right\} = 0 \quad (20)$$

where σ_I represents the uncertainty of data point $Y_m(I\Delta\tau)$ with the subscript m denoting the measured value, and the net signal autocorrelation function $Y(I\Delta\tau)$ [$=A\beta|g^{(1)}(I\Delta\tau)|^2$] has the form

$$Y(I\Delta\tau) = A\beta\left\{\sum_{j=1}^{n} a_j\left[-\frac{1}{I\Delta\tau}\right] \times \right.$$
$$\left.[\exp(-(\Gamma j + \Delta\Gamma/2)I\Delta\tau) - \exp(-(\Gamma_j - \Delta\Gamma/2)I\Delta\tau)]\right\}^2 \quad (21)$$

with $A\beta$ being another unknown parameter in the data fitting procedure. We used a range of n such that $Y(I\Delta\tau)$ and $Y_m(I\Delta\tau)$ agree to within statistical counting error limits.

In order to obtain the normalized number distribution $f(M)$ from $G(\Gamma)$, we first transform the discrete limits in Γ space to the corresponding values in M space. For Γ_{j1} ($=\Gamma_j - \Delta\Gamma/2$) and Γ_{j2} ($=\Gamma_j + \Delta\Gamma/2$), we get M_{j1} and M_{j2} by means of eq 16 if b is known. It should be noted that the corresponding histogram steps in M space are no longer of equal magnitude with

$$\Delta M_j = \text{abs}(M_{j2} - M_{j1}) \quad (22)$$

$$\bar{M}_j = (M_{j2} + M_{j1})/2 \quad (23)$$

In M space, we can transform $G(\Gamma)\, d\Gamma$ such that $G(\Gamma)\, d\Gamma$ becomes $M^2P(M)f^*(M)M^{-(b+1)}\, dM$ where $f(M) = f^*(M)/\sum f^*(M)\Delta M_j$. The particle scattering factor $P(M)$ can be approximated by taking $P(X) = 2(e^{-X^2} - 1 + X^2)/X^4$, where $X = Kr_g$. In assuming the random coil behavior for the scattering factor $P(X)$, we have also set

$$\bar{r}_g \text{ (at infinite dilution)} \approx \frac{k_B T}{6\pi\eta 0.665}\frac{\bar{M}^b}{k_T} \quad (24)$$

Thus, at a fixed K,

$$f^*(\bar{M}_j) = \frac{G(\Gamma_j)\Delta\Gamma_j}{\bar{M}_j^{1-b}P(\bar{M}_j)\Delta M_j} \quad (25)$$

Equations 25, 23, 16, and 15 permit us to transform the histogram in Γ space for a determination of the molecular weight distribution function provided that b is known. Conversely, if we determine a weight-average molecular weight M_r by means of light-scattering intensity measurements, we can match the measured M_r with M_r computed from a plot of $f(M)$ vs. M and, in principle, estimate the value of b. In practice, such an estimate for b becomes meaningful only for resonably narrow molecular weight distribution functions where the approximation for a constant k_D, independent of molecular weight, remains valid.

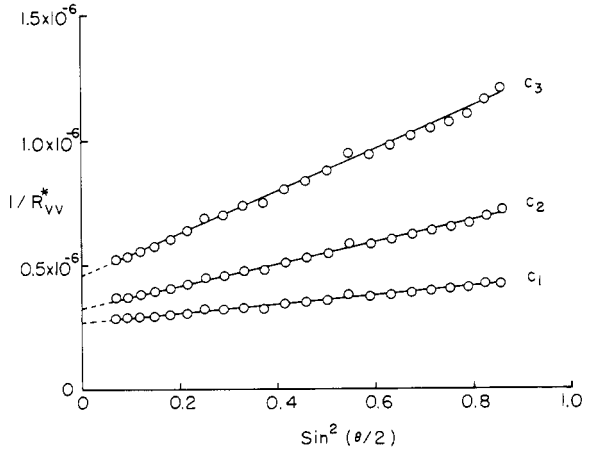

Figure 1. Plots of reciprocal relative excess Rayleigh ratio ($1/R_{vv}^*$) vs. $\sin^2(\theta/2)$ at three different concentrations for poly[bis(*m*-chlorophenoxy)phosphazene] in chloroform: $C_1 = 2.546$ mg/g, $C_2 = 1.202$ mg/g, $C_3 = 0.610$ mg/g; $\lambda_0 = 488.0$ nm; $t = 25$ °C.

Table I
Concentration Dependence of Radii of Gyration $\langle r_g^2(C)\rangle_z^*$ and $\langle r_g^2(C)\rangle_z$ for Poly[bis(*m*-chlorophenoxy)phosphazene] (sample IIIe in ref 4) in Chloroform at 25 °C

concn, mg/g	$(\langle r_g^2(C)\rangle_z^*)^{1/2}$, Å	$(\langle r_g^2(C)\rangle_z)^{1/2}$,[a] Å
2.546	696	1.50×10^3
1.202	962	1.58×10^3
0.610	1125	1.54×10^3
∞ dilution	(1.24×10^3)	1.54×10^3

[a] $\langle r_g^2(C)\rangle_z = \langle r_g^2(C)\rangle_z^*(1 + 2A_2CM_r)^{1/2} = \langle r_g^2(C)\rangle_z^*(1 + 9.59 \times 10^2\, C)^{1/2}$ with C expressed in g/cm³. Density of chloroform = 1.47985 g/cm³ at 25 °C and we have taken $A_2 = 1.39 \times 10^{-4}$ (cm³ mol)/g² and $M_r = 3.45 \times 10^6$ g/mol, which compared favorably with $M_r = 3.56 \times 10^6$ g/mol from GPC.[18]

V. Results and Discussion

We used benzene as a reference[16] for computing the Rayleigh ratio and took $R_{vv}^B(\theta = 90°) = 3.26 \times 10^{-5}$ cm^{-1} for $\lambda_0 = 488.0$ nm at 30 °C. With

$$(R_{vv}^B)_t = (R_{vv}^B)_{25}(1 + 0.368 \times 10^{-2}(t - 25\ °C)) \quad (26)$$

where t is temperature expressed in °C, we obtained $(R_{vv}^B)_{25} = 3.20 \times 10^{-5}$ cm^{-1}. From the benzene reference, we computed an instrument constant Q for our light-scattering photometer, such that $Q = R_{vv}/R_{vv}^* = 2.633 \times 10^{-10}$. Thus, all absolute Rayleigh ratios of this study correspond to $R_{vv} = 2.633 \times 10^{-10}R_{vv}^*$.

Figure 1 shows plots of $1/R_{vv}^*$ vs. $\sin^2(\theta/2)$ at concentrations $C_1 = 2.546$ mg/g, $C_2 = 1.202$ mg/g, and $C_3 = 0.610$ mg/g. By taking $n_0 = 1.4429$ and $\lambda_0 = 488.0$ nm and by measuring $dn/dC = 0.120$ cm³/g with a Rayleigh interferometer, we obtained $H = 3.47 \times 10^{-7}$ (cm²/g)² mol. Table I lists the result of $\langle r_g^2(C)\rangle_z^*$ as a function of concentration by means of eq 5 and 7. The apparent radius of gyration $\langle r_g^2(C)\rangle_z^*$ has a large concentration dependence because of the $(1 + 2A_2CM_r)$ term, as shown in Figure 2 where we would have obtained an incorrect radius of gyration (1240 ± 30 Å) by linear extrapolation to infinite dilution. Figure 3 shows a plot of $\lim_{\theta\to 0}(C/R_{vv}^*)$ vs. concentration. We obtained $M_r = Q/(H\cdot\text{intercept}) = (3.45 \pm 0.24) \times 10^6$ g/mol and $A_2 = (1.39 \pm 0.04) \times 10^{-4}$

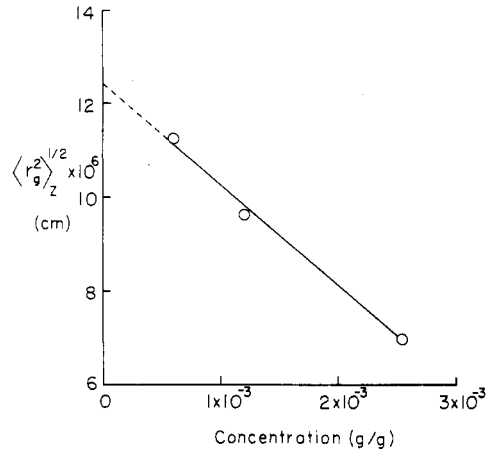

Figure 2. Plot of $(\langle r_g^2 \rangle_z^*)^{1/2}$ vs. concentration for poly[bis(*m*-chlorophenoxy)phosphazene] in chloroform at 25 °C. $\langle r_g^2(C) \rangle = \langle r_g^2(C) \rangle_z^*(1 + 9.59 \times 10^2 C)^{1/2}$, with C expressed in g/cm³.

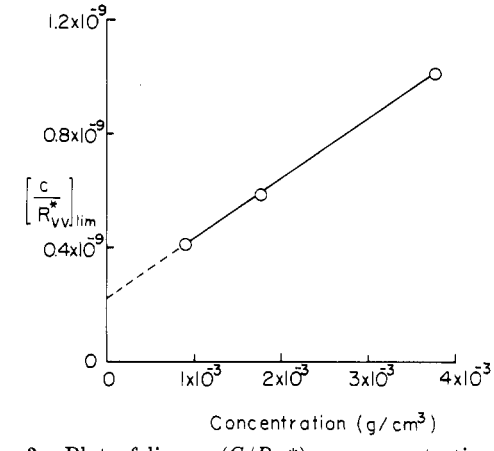

Figure 3. Plot of $\lim_{\theta \to 0} (C/R_{vv}^*)$ vs. concentration. $M_r = Q/(H \cdot \text{intercept}) = (3.45 \pm 0.24) \times 10^6$ g/mol; $A_2 = \text{slope} \cdot H/2Q = (1.39 \pm 0.04) \times 10^{-4}$(cm³ mol)/g².

Table II
Concentration Dependence of $\bar{D}$ ($=\bar{\Gamma}/K^2$) and $\mu_2/\bar{\Gamma}^2$ (eq 17) for Poly[bis(*m*-chlorophenoxy)phosphazene] (M_r = 3.45 × 10⁶ g/mol) in Chloroform at θ = 90° and 25 °C

concn, mg/g	$\bar{D} \times 10^7$,[a] cm²/s	$\mu_2/\bar{\Gamma}^2$
0.610	1.502 ± 0.007	0.75 ± 0.02
1.202	1.590 ± 0.007	0.80 ± 0.02
2.546	1.815 ± 0.007	0.84 ± 0.04
∞	1.40 ± 0.01	

[a] $D \approx D_0(1 + 116C)$ with C expressed in g/g of solution.

(cm³ mol)/g². It is important to note that $\langle r_g^2(C) \rangle_z$ is relatively independent of concentration, and we estimated $\langle r_g^2 \rangle_z$ to be 1.54 × 10³ Å.

In line-width studies, we first used the method of cumulants[17] to compute $\bar{D}$ ($=\bar{\Gamma}/K^2$) and $\mu_2/\bar{\Gamma}^2$. Table II lists the concentration dependence of $\bar{D}$ and $\mu_2/\bar{\Gamma}^2$ (eq 17) for sample IIIe of ref 4 in chloroform at θ = 90° and 25 °C. Figure 4 shows a plot of $\bar{D}$ vs. concentration. The intercept corresponds to $\bar{D}_0 = 1.40 \times 10^{-7}$ cm²/s, and the slope yields k_D = 116 g of solution/g or 116/1.4799 = 78.4 cm³/g by means of eq 8. If we take $1/\bar{v}$ = 1.25 g/cm³, b = 0.57, $k_T = 2.08 \times 10^{-4}$ (cm²/s)(g/mol)$^{0.57}$, and F = 1.0, we can compute k_D from eq 12, which gives k_D = 159 cm³/g. In eq 12, k_D is the difference of two large numbers, and the assignment of F is uncertain. Thus, we prefer to use the experimentally determined k_D.

In Table II, we should note that the variance $\mu_2/\bar{\Gamma}^2$ has values greater than 0.5, which suggests the presence of a

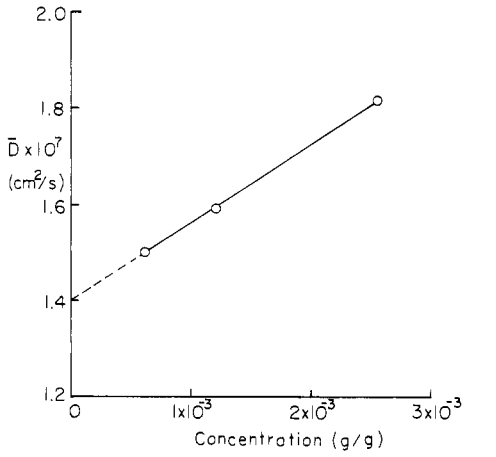

Figure 4. Plot of $\bar{D}$ vs. concentration (g/g) at θ = 90° and 25 °C. $\bar{D}_0$ = intercept = 1.40 × 10⁻⁷ cm²/s; k_D = slope = 116 g of solution/g or 78.4 cm³/g.

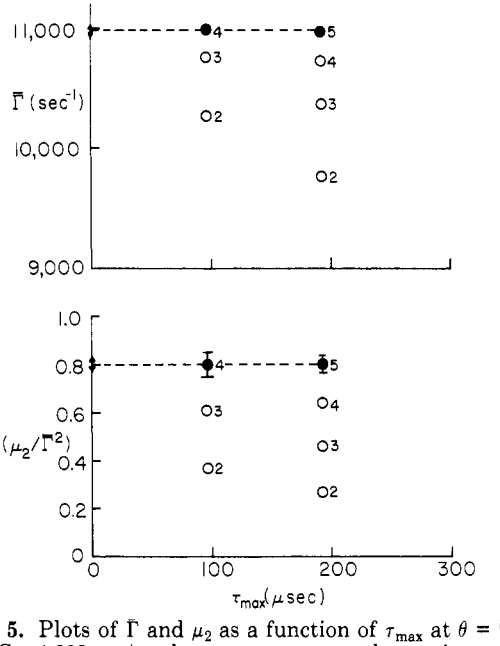

Figure 5. Plots of $\bar{\Gamma}$ and μ_2 as a function of τ_{max} at θ = 90°, t = 25 °, C = 1.202 mg/g, where τ_{max} represents the maximum delay time used. We used two delay times (1 and 2 μs) so that we could take advantage of 96 data points for each fit. The extrapolated values of $\bar{\Gamma}$ and $\mu_2/\bar{\Gamma}^2$ from fourth and fifth order cumulants fit are in agreement with values computed based on $G(\Gamma)$ of Figure 7 (solid histogram) obtained by the histogram method.

bimodal distribution. In the cumulants method, we have also taken particular care to obtain the correct $\bar{\Gamma}$ and μ_2 values because an extrapolation procedure is required whenever the line-width distribution yields large variances. Figure 5 shows plots of $\bar{\Gamma}$ and μ_2 as a function of $\bar{\Gamma}\tau_{max}$ where τ_{max} represents the maximum delay time used in the computation by means of various orders of cumulants expansion. The usual quadratic (second order to the μ_2 term) fit does not give correct answers even for $\bar{\Gamma}$, except in the limit $\bar{\Gamma}\tau_{max} \to 0$. A slight increase in $\mu_2/\bar{\Gamma}^2$ at increasing concentrations can be attributed to the concentration dependence of Γ. The measured self-beating single-clipped autocorrelation function has the form

$$G_k^{(2)}(I\Delta\tau) = A(1 + \beta|g^{(1)}(I\Delta\tau)|^2) \qquad (27)$$

where k is the clipping level, A is the background, and β is an adjustable parameter. Figure 6 shows a plot of net signal autocorrelation function $A\beta|g^{(1)}(\tau)|^2$ as a function of delay channel number I at C_2 = 1.202 mg/g, θ = 90°, t = 25 °C, and $\Delta\tau$ = 2 μs. We used the nonlinear least-squares

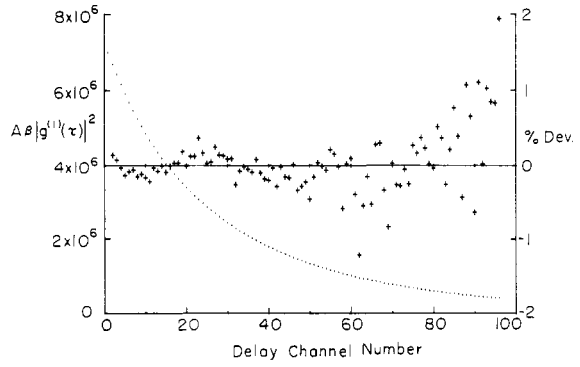

Figure 6. Plots of $A\beta|g^{(1)}(\tau)|^2$ and percent deviation vs. delay channel number I. Dots denote $A\beta|g^{(1)}(\tau)|^2$; crosses denote percent deviation (% dev)

$$\%\ \text{dev} = 100\left[\frac{Y_m(I\Delta\tau) - Y(I\Delta\tau;\text{eq 21})}{Y_m(I\Delta\tau)}\right]$$

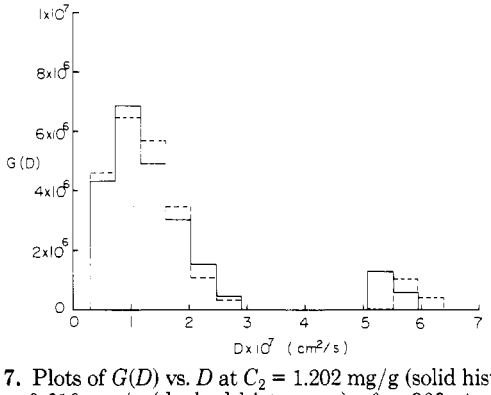

Figure 7. Plots of $G(D)$ vs. D at $C_2 = 1.202$ mg/g (solid histogram) and $C_3 = 0.610$ mg/g (dashed histogram): $\theta = 90°$, $\Delta\tau = 2$ μs.

method (eq 20) to obtain the histogram approximation according to eq 18 and 19 with percent deviation (Figure 6) agreeing to within the statistical error limits. Instead of $G(\Gamma)$ vs. Γ, we have converted Γ to D by means of $D = \Gamma/K^2$. Figure 7 shows plots of $G(D)$ vs. D at $C_2 = 1.202$ mg/g (solid histogram) and $C_3 = 0.610$ mg/g (dashed histogram), $\theta = 90°$, and $\Delta\tau = 2$ μs. The agreement between the solid and dashed histograms is to be expected since the concentration variation corresponds to about a 7% change. Nevertheless, it is important to remember that even at dilute concentrations, eq 14 is a useful way to correct for the concentration effect on the diffusion coefficient.

In a proper conversion from Γ space to M space, we used eq 16 to convert each Γ step to M step in the X axis and $G(\Gamma)\ d\Gamma$ to $M^2P(M)f^*(M)M^{-(b+1)}\ dM$ with

$$r_g = k_r M^b \tag{28}$$

and the particle scattering factor assumed to obey random coil behavior. If we take $r_g = 1.54 \times 10^3$ Å and $M_r = 3.45 \times 10^6$ g/mol from intensity measurements and $b = 0.57$, we obtain $k_r = 2.89 \times 10^{-9}$ cm/(g/mol)$^{0.57}$, which compares favorably with $k_r = 2.91 \times 10^{-9}$ cm/(g/mol)$^{0.57}$ computed by means of eq 24 using $k_T = 2.08 \times 10^{-4}$ (cm^2/s)(g/mol)$^{0.57}$ and $\eta = 0.00542$ P.

Figure 8 shows plots of $f(M)$ versus ln M. In the upper plots, the solid histogram represents results from $C_2 = 1.202$ mg/g with $b = 0.57$ and the dashed histogram represents results from $C_3 = 0.610$ mg/g with $b = 0.57$. By matching the $M_r = 3.45 \times 10^6$, which is invariant, we obtained $k_T = 2.02 \times 10^{-4}$ (cm^2/s)(g/mol)$^{0.57}$ and 2.14×10^{-4}(cm^2/s)(g/mol)$^{0.57}$ at $C_2 = 1.202$ mg/g and $C_3 = 0.610$ mg/g, respectively. The 5% agreement is within the error limits of our histogram approximation. Two scales were

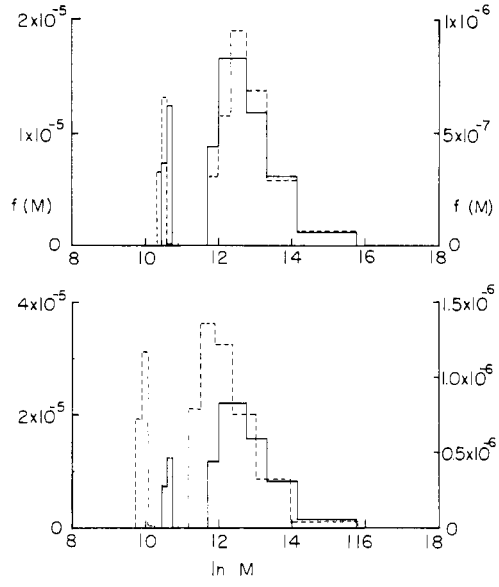

Figure 8. Plots of $f(M)$ vs. ln M. Left scale denotes the low molecular weight fraction and right scale the high molecular weight fraction. Set I (above): Solid histogram—$C_2 = 1.202 \times 10^{-3}$ g/g, M_r(matched) $= 3.45 \times 10^6$ g/mol, $k_T = 2.02 \times 10^{-4}$ (cm^2/s)(g/mol)$^{0.57}$, and $b = 0.57$. Dashed histogram—$C_3 = 0.610 \times 10^{-3}$ g/g, $M_r = 3.45 \times 10^6$ g/mol, $k_T = 2.14 \times 10^{-4}$ (cm^2/s)(g/mol)$^{0.57}$, and $b = 0.57$. Set II (below): Solid histogram—$C_2 = 1.202 \times 10^{-3}$ g/g, M_r(matched) $= 3.45 \times 10^6$ g/mol, $k_T = 2.02 \times 10^{-4}$ (cm^2/s)(g/mol)$^{0.57}$, and $b = 0.57$. Dashed histogram—$C_2 = 1.202 \times 10^{-3}$ g/g, $M_r = 3.45 \times 10^6$ g/mol, $k_T = 6.84 \times 10^{-5}$ (cm^2/s)(g/mol)$^{1/2}$, and $b = 0.50$.

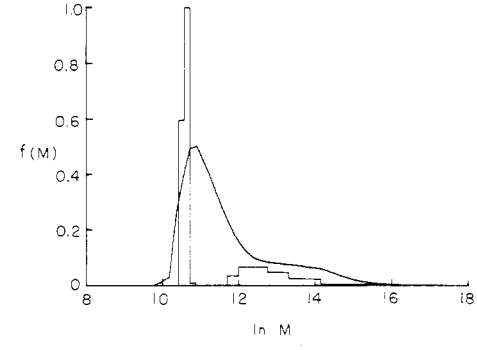

Figure 9. Plots of $f(M)$ vs. ln M. The light-scattering result with $C_2 = 1.202$ mg/g, $b = 0.57$, and $k_T = 2.02 \times 10^{-4}$ (cm^2/s)(g/mol)$^{0.57}$ is represented by the histogram; the GPC result from ref 6 is represented by the solid curve.

used for the bimodal distribution with the low molecular weight fraction denoted by the 10^{-5} range. Hagnauer and LaLiberte[18] determined the intrinsic viscosity–molecular weight relationship in chloroform at 25 °C to be $[\eta] = 6.27 \times 10^{-5}M^{0.70}$ dL/g. If we used the Scheraga–Mandelkern[19] relation $1 + \alpha = 3b$, we obtained $b = 1.7/3 = 0.57$, in agreement with b from our molecular weight distributions determined at two different concentrations. It should be noted that our transform is sensitive to the value of b. In the lower plots of Figure 8, we can see that the distribution function would have been shifted markedly if we used $\beta = 0.50$ at the same concentration. In Figure 9, we made a direct comparison of our histogram results with that from GPC.[6] There is no adjustable parameter except for the value b which has been checked by intrinsic viscosity studies.

In summary, we have devised a new practical approach for the determination of molecular weight distribution functions by means of photon-correlation spectroscopy and histogram method of data analysis. We have outlined a general method for the transform from Γ space to M space

and have illustrated our method by using a poly[bis(*m*-chlorophenoxy)phosphazene] sample of known molecular weight distribution function. We have confirmed the bimodal distribution function of sample IIIe as determined by GPC analysis. Indirectly, we have also confirmed $b = 0.57$ for poly[bis(*m*-chlorophenoxy)phosphazene] in chloroform at 25 °C. A salient feature of our approach is the range of its applicability, since quasielastic light scattering can routinely measure diffusion coefficients from 10^{-6} to 10^{-9} cm^2/s. Thus, molecular weight distribution functions from 10^3 to 10^9 can be determined. Furthermore, only very small quantities of the solution are required to carry out the study and the measurement time is fairly short, in minutes under most circumstances.

Acknowledgment. We are grateful for the support of this research by the U.S. Army Research Office and to Dr. G. L. Hagnauer of the Army Materials and Mechanics Research Center, Watertown, Mass., for furnishing us with the poly[bis(*m*-chlorophenoxy)phosphazene] (sample IIIe). Initial studies of sample IIIe in chloroform were performed by Y. Tsunashima.

References and Notes

(1) H. R. Allcock, R. L. Kugel, and K. J. Valan, *Inorg. Chem.*, **5**, 1709 (1966).
(2) H. R. Allcock, "Phosphorus-Nitrogen Compounds", Academic Press, New York, 1972.
(3) H. R. Allcock, *Chem. Rev.*, **72**, 315 (1972).
(4) R. E. Singler, G. L. Hagnauer, N. S. Schneider, B. R. LaLiberte, R. E. Sacher, and R. W. Matton, *J. Polym. Sci., Part A-1*, **12**, 433 (1974).
(5) R. E. Singler, N. S. Schneider, and G. L. Hagnauer, *Polym. Eng. Sci.*, **15**, 321 (1975).
(6) G. L. Hagnauer and B. R. LaLiberte, *J. Polym. Sci., Polym. Phys. Ed.*, **14**, 367 (1976).
(7) Courtesy of Dr. G. L. Hagnauer, Army Materials and Mechanics Research Center, Watertown, Mass. 02172.
(8) M. Kerker, "The Scattering of Light and Other Electromagnetic Radiation", Academic Press, New York, 1969.
(9) H. Yamakawa, "Modern Theory of Polymer Solutions", Harper and Row, New York, 1971.
(10) C. W. Pyun and M. Fixman, *J. Chem. Phys.*, **41**, 937 (1964).
(11) H. Yamakawa, *J. Chem. Phys.*, **36**, 2295 (1962).
(12) S. Imai, *J. Chem. Phys.*, **50**, 2116 (1969).
(13) F. C. Chen, A. Yeh, and B. Chu, *J. Chem. Phys.*, **66**, 1290 (1977).
(14) Y. Tsunashima, K. Moro, and B. Chu, *Biopolymers*, **17**, 251 (1978).
(15) B. Chu, Esin Gulari, and Erdogan Gulari, *Phys. Scr.*, in press.
(16) J. Ehl, C. Loucheux, C. Reiss, and H. Benoit, *Makromol. Chem.*, **75**, 35 (1964).
(17) D. E. Koppel, *J. Chem. Phys.*, **57**, 4814 (1972).
(18) G. L. Hagnauer and B. R. LaLiberte, *J. Appl. Polym. Sci.*, **20**, 3073 (1976); G. L. Hagnauer, B. R. LaLiberte, R. E. Singler, S. J. Kaplan, and E. R. Plumer, "Macromolecular Characterization of Poly[bis(*m*-chlorophenoxy)phosphazene]", AMMRC TR 76-25 (1976).
(19) H. A. Scheraga and L. Mandelkern, *J. Am. Chem. Soc.*, **75**, 179 (1953).

Small-Angle X-ray Scattering from Block Polymers. 3. Random Phase Approximation

A. D. LeGrand† and D. G. LeGrand*

General Electric Company Corporate Research and Development Chemical Laboratory, Schenectady, New York 12301. *Received December 26, 1978*

ABSTRACT: The random phase approximation (RPA) is used in the development of the theory for small-angle X-ray scattering from block copolymers which have not undergone microphase separation. Explicit expressions for the intensity of scattering as a function of scattering angle are presented for di-, tri-, and pentablock polymers and are shown to exhibit a reciprocity relation. Calculated scattering curves as a function of angle are presented for a variety of triblock structures, and it is suggested that the calculated maxima in some of the curves reflect the superposition of the RPA and a Debye function.

Information pertaining to the molecular structure of block polymers, both in dilute solution and the bulk state, is important in the development of a better understanding and an efficient use of such materials. In previous studies, we have calculated the expected small-angle X-ray scattering (SAXS) behavior of block polymers in dilute solutions and in the structured bulk state.[1,2] In these works, we adopted and extended the classic concepts and works of Debye. Recently, deGennes has proposed the use of the random phase approximation (RPA) in attempting to explain the X-ray scattering behavior of mono- and dihalogenated alkanes as presented by Brady and Coworkers.[3-6] At the suggestion of deGennes and our own interest in developing alternate models to predict the SAXS of block polymers, we have explored the use of RPA in calculating the SAXS from block polymers in the bulk state. It is believed that this model should be applicable to block polymers where microphase separation is not expected due to either small differences in cohesive energy density or the size of the comonomeric blocks is so small that geometric restrictions alone ensure random mixing.

† Physics Department, Brown University, Rhode Island.

Theory

We assume that the block polymer molecules are monodisperse in structure, composition, and molecular weight. As shown elsewhere, the expected SAXS intensity for a dilute solution would be given as

$$I(\mathbf{q}) = k_B T \sum\sum \alpha_i \chi_{ij}^0(\mathbf{q}) \alpha_j \tag{1}$$

where α_i is the scattering amplitude for the ith monomer, $\mathbf{q}$ is the scattering wave vector, and $\chi_{ij}^0(\mathbf{q})$ is a response function and is proportional to the pair correlation function $P_{ij}^0(\mathbf{r})$ for two species on the chain.[1] For an ideal coil, $\chi_{ij}^0(\mathbf{r})$ is given by

$$\chi_{ij}^0(\mathbf{r}) = \frac{\rho}{N k_B T} P_{ij}^0(\mathbf{r}) \tag{2a}$$

$$\chi_{ij}^0(\mathbf{r}) = \frac{\rho}{N k_B T} \frac{3}{(2\pi|i-j|\sigma^2)^2} \exp\left(-\frac{3r^2}{2|i-j|\sigma^2}\right) \tag{2b}$$

When interactions between the species are taken into account by the use of the RPA (a brief discussion behind the use and physics of the RPA is presented in the Appendix), then instead of eq 1, one obtains[3]

0024-9297/79/2212-0450$01.00/0